Effects of ginsenoside Rg1 on HIF-1a, VEGF, and ET-1 expression in mice with chronic intermittent hypoxia and pain

Fei QIN[1] , Peng WANG[2] , Min ZHANG[3] , Zhang QIANGZE[1] , Zhuang HE[4] , Bing LIU[5]*

Abstract

Chronic intermittent hypoxia (CIH) is associated with pulmonary hypertension and lacks effective early intervention approaches. Our study intends to investigate the protective effect of ginsenoside Rg1 on pulmonary small artery damage of CIH in mice. A total of 72 SPF-grade male C57BL/6 mice were randomly divided into an experimental group, which received ginsenoside Rg1 10 mg/kg (low-dose group, group T1) and 20 mg/kg (high-dose group, group T2) daily, and the control group (group C), which received an equal volume of normal saline every day. Samples were collected on days 7, 10, and 14 after treatment to assess HIF-1a, VEGF, and ET-1 levels by immunohistochemical staining, serum level of HIF-1a, VEGF, and ET-1 by ELISA, or the mRNA level of HIF-1a, VEGF, and ET-1 by real-time PCR. The control group presented increased serum levels of HIF-1a, VEGF, and ET-1 from days 7 to 14. Compared with the control group, the treatment group showed significantly decreased serum levels of HIF-1a, VEGF, and ET-1 on day 7, 10, or 14 at the same time points ($P < 0.05$). Consistently, immunohistochemical staining analysis also showed an increased trend of HIF-1a, VEGF, and ET-1 IOD values in the control group, which were all decreased in the treatment group at the same time points with the lower level in the T2 group than the T1 group ($P < 0.05$). Moreover, HIF-1a, VEGF, and ET-1 mRNA levels in groups C, T1, and T2 also showed similar results to immunohistochemical staining ($P < 0.05$ or $P < 0.001$). In the treatment group, HIF-1a was positively correlated with VEGF or ET-1 and VEGF was positively correlated with ET-1. Ginsenoside Rg1 inhibits the expression of HIF-1a, VEGF, and ET-1 in mice with CIH and pain.

Keywords: Chronic intermittent hypoxia; sleep apnea syndrome; ginsenoside Rg1; HIF-1a; VEGF; ET-1.

Practical Application: Obstructive sleep hypopnea syndrome (OSAHS) is a common type of sleep apnea syndrome. Chronic intermittent hypoxia (CIH) can cause pathophysiological changes in the body, leading to multi-organ damage, especially cardiovascular and cerebrovascular diseases. This study demonstrated that ginsenoside Rg1 inhibits the expression of HIF-1a, VEGF, and ET-1 in mice with CIH and pain.

1 INTRODUCTION

Obstructive sleep hypopnea syndrome (OSAHS) is a common type of sleep apnea syndrome. CIH can cause pathophysiological changes in the body, leading to multi-organ damage, especially cardiovascular and cerebrovascular diseases (Amsen et al., 2004; An et al., 2011). OSAHS is closely associated with the onset of pulmonary hypertension, hypertension, coronary atherosclerotic heart disease, and stroke (Ajoolabady et al., 2023; Akatsuka, 2020).

Chronic hypoxia is capable of inducing pulmonary vascular remodeling, resulting in pulmonary hypertension and right ventricular hypertrophy. Chronic hypoxic pulmonary hypertension is featured as a sustained increase in the pulmonary arterial pressure possibly due to abnormally elevated pulmonary vascular resistance. It is a potentially severe and fatal lung disorder that develops in patients with chronic lung disease including chronic obstructive pulmonary disease (Askenase, 2021; Aversa et al., 2016). Among several dysregulated signaling pathways during hypoxic pulmonary hypertension, hypoxia-induced factor (HIF) signaling is critical to the disease progression not only in pulmonary arterial hypertension (PAH) (Antonarakis et al., 2014) but also in PH due to lung diseases and/or hypoxia, including PH associated with chronic high altitude exposure (Huang et al., 2019; Huang et al., 2020), chronic obstructive pulmonary disease (COPD) (Dłuski et al., 2022), and PF (Askenase, 2021) (group III PH). HIF-1 and HIF-2 play dominant roles in the regulation of gene expression in response to hypoxia. Under normoxic conditions, degradation of HIF-1α is initiated by hydroxylation

of conserved proline residues (Galluzzi et al., 2020; Versteijne et al., 2020). However, during hypoxia, HIF-1α degradation is inhibited, leading to its accumulation, dimerization with HIF-1β, and subsequent activation of hypoxia-specific genes (Poher et al., 2018). HIF-dependent genes can modulate a wide range of processes *in vivo* including vascular endothelial growth factor (VEGF)-induced vascularization, erythropoiesis, cellular proliferation and migration, and cellular energy and metabolism (Jeon et al., 2022; Perner & Krüger, 2022).

Ginsenoside Rg1 is one of ginseng's main active drug ingredients and Panax notoginseng (Baimas-George et al., 2021). Pharmacological studies have found that ginsenoside Rg1 possesses various bioactive properties, such as anti-oxidative stress, anti-inflammatory, and anti-apoptosis. Injections with ginseng as the main drug, such as Shenmai injection, Shengmai injection, and Shenqi injection, have been widely utilized to treat cardiovascular and cerebrovascular diseases for a long time. However, whether ginsenoside Rg1 has a protective effect on CIH-induced lung injury remains poorly understood. Our study aims to explore the effect of ginsenoside Rg1 in chronic lung injury induced by CIH.

2 MATERIALS AND METHODS

2.1 Establishment of CIH model and animal grouping

A total of 72 SPF male C57BL/6 mice with a body mass of 20–22 g were purchased from the Laboratory Animal Center of Fujian Medical University [SCXK (Fujian) 2012-0001]. In the homemade gas program control box, the oxygen concentration in each cycle was maintained between $6 \pm 1\%$ and $21 \pm 1\%$ by oxygen monitor, and the CIH mice model was established after 30 days of intermittent hypoxia (Zaibi et al., 2021).

The purity of ginsenoside Rg1 (ginsenoside Rg1 (CAS No. 22427-39-0) provided by Shanghai Jinye Biotechnology Co, Ltd.) was 98.1%. After model establishment, 72 mice from the hypoxic group were randomly divided into a low-dose treatment group (10 mg/kg, T1), a high-dose treatment group (20 mg/kg, T2), and a control group (group C) using random numbers. Samples were taken on days 7, 10, and 14.

2.1.1 H&E staining

After 30 days of intermittent hypoxia, eight mice were taken on days 7, 10, and 14 after ginsenoside Rg1 treatment for blood collection. Then, the chest was cut up along the thorax, and the left lung tissue of mice was obtained and fixed in 40 g/L neutral formaldehyde for 1 week for H&E staining. The right lung tissue was placed in a frozen tube in liquid nitrogen and transferred to a -80°C refrigerator for further use.

The left lung tissue specimen fixed in 10% neutral formalin was removed, routinely dehydrated, paraffin-embedded, and continuously sectioned with 4 μm thickness. After eosin and elastic fiber were stained, the pathological changes were observed under a light microscope, and the results were analyzed using the image analysis software (Image-pro plus 6.0). Three lung tissue sections were randomly selected for each mouse to measure the thickness of the intima and membrane.

2.2 Immunohistochemical staining of the lung tissue

This assay was performed using the SABC/DAB method in the paraffin sections in accordance with the protocols. Three sections with complete structures, each with five pulmonary arterioles of about 100 m in diameter, were randomly selected, and one image with 400′ magnification was taken at the specific expression site. The mean absorbance values of the photographs were analyzed by the IPP6 software.

2.3 qRT-PCR

RNA was isolated from lung tissues to measure the expression levels of HIF-1a mRNA, VEGF mRNA, and ET-1 mRNA by quantitative real-time PCR. Gene expression was analyzed using the 2^{-Ct} method. The primer sequences are shown in Table 1.

2.4 ELISA

Serum was isolated from mice after different treatments to measure the levels of HIF-1a, VEGF, and ET-1 by ELISA according to the instructions.

2.5 Statistical methods

The SPSS 26.0 statistical package was utilized to analyze the data that were displayed as mean ± SD and assessed by one-way ANOVA. $P < 0.05$ indicates a significance.

3 RESULTS

3.1 Comparison of serum HIF-1a, VEGF, and ET-1 levels in each group

Serum concentrations of HIF-1a, VEGF, and ET-1 continued to increase in the control group, while their levels decreased in the treatment group and tended to decrease over time ($P < 0.05$) (Table 2). In addition, the T2 group had significantly lower serum levels of VEGF and ET-1 than the T1 group at the same time point ($P < 0.001$).

3.2 Correlation analysis of HIF-1a, VEGF, and ET-1 in the treatment group

Serum HIF-1a and ET-1 levels were positively correlated in the treatment group. HIF-1a was positively correlated with VEGF, and VEGF was positively associated with ET-1 (Table 3).

Table 1. Primer sequences.

Primer name	Primer sequences (5'–3')
MusACTB_qF	TGCTGTCCCTGTATGCCTCTG
MusACTB_qR	TTGATGTCACGCACGATTTCC
MusHIF-1aa_qF	TTCTCCAAGCCCTCCAAGTATG
MusHIF-1aa_qR	TGATGCCTTAGCAGTGGTCGTT
MusET-1_qF	TGTTCCCTAGCCTGTCTGCG
MusET-1_qR	TCGCCCTGCTGTGGAATCTC
MusVEGF_qF	TGTCACCACCACGCCATCA
MusVEGF_qR	ACGAATCCAGTCCCACGAGG

3.3 Comparison of HIF-1a, VEGF, and ET-1 expressions in the lung tissues

The IOD values of HIF-1a, VEGF, and ET-1 as measured by immunohistochemical staining (Figure 1) in the control group continued to increase after model establishment, while their IOD values decreased in the treatment group and tended to decrease over time with a significant difference ($P < 0.001$) (Table 3). In addition, the T2 group had significantly lower levels of HIF-1a, VEGF, and ET-1 than the T1 group at the same time point ($P < 0.001$) (Table 4).

**Table 2**. Comparison of serum HIF-1a, VEGF, and ET-1 concentrations in mice of each group (pg/mL, $n = 8$).

	Group	Day 7	Day 10	Day 14
HIF-1a	C group	17.27 ± 1.83	17.57 ± 1.59	18.90 ± 1.91
	T1 group	$15.45 \pm 1.94^*$	$13.27 \pm 2.31^*$	$13.66 \pm 2.61^*$
	T2 group	$13.82 \pm 2.42^*$	$13.21 \pm 2.46^*$	$13.49 \pm 2.24^*$
VEGF	C group	13.94 ± 2.79	13.92 ± 2.23	14.12 ± 2.00
	T1 group	$10.79 \pm 1.69^*$	$10.42 \pm 1.72^*$	$9.34 \pm 0.94^*$
	T2 group	$8.06 \pm 1.52^{*\triangle}$	$7.08 \pm 1.40^{*\triangle}$	$6.33 \pm 1.10^{*\triangle}$
ET-1	C group	46.30 ± 1.45	46.35 ± 0.94	47.45 ± 2.35
	T1 group	$42.50 \pm 1.18^*$	$40.48 \pm 2.44^*$	$40.80 \pm 2.20^*$
	T2 group	$39.37 \pm 2.05^{*\triangle}$	$36.44 \pm 2.30^{*\triangle\square}$	$36.64 \pm 2.03^{*\triangle\square}$

Compared with the C group, $^*P < 0.001$; compared with the T1 group; $^\triangle P < 0.001$; $^\square P > 0.05$.

Table 3. Correlation of HIF-1a, VEGF, and ET-1 in the treatment groups.

Project	Day 7		Day 10		Day 14	
	r	P	r	P	r	P
HIF-1a and VEGF	0.366	0.086	0.497*	0.019	0.607*	0.002
HIF-1a and ET-1	0.424*	0.044	0.527*	0.013	0.0715*	< 0.001
VEGF and ET-1	0.698*	< 0.001	0.726*	< 0.001	0. 853*	< 0.001

*Correlation coefficient, $P < 0.05$ or $P < 0.001$.
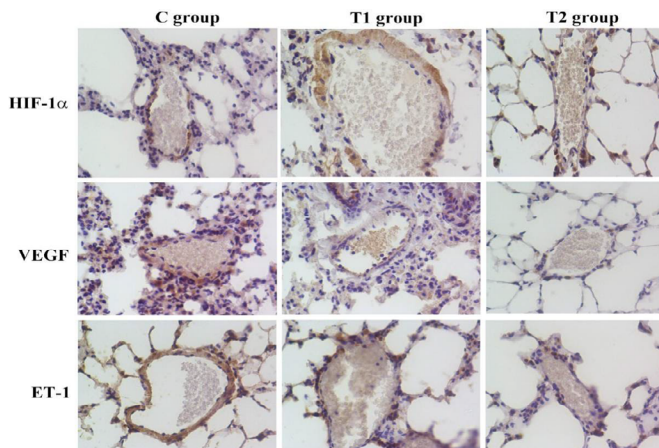
Figure 1. Immunohistochemical staining of HIF-1a, VEGF, and ET-1 in mouse lung tissue on day 7.

3.4 Correlation analysis of HIF-1a, VEGF, and ET-1 expression in the treatment group

In the treatment group, HIF-1a was positively correlated with VEGF or ET-1, and VEGF was positively correlated with ET-1 (Table 5).

3.5 Comparison of mRNA level of HIF-1a, VEGF, and ET-1 in the mouse lung tissue

The average absorbance ratio of mRNA level of HIF-1a, VEGF, and ET-1 was increased in the control group from days 7 to 14 (Table 6). However, the ratio was significantly decreased in the treatment group compared with the control group at the same time point with a tendency to decrease over time ($P < 0.001$). Moreover, the T2 group had a significantly lower ratio of HIF-1a, VEGF, and ET-1 mRNA than the T1 group at the same time point ($P < 0.001$) (Table 6).

Table 4. Comparison of HIF-1a, VEGF, and ET-1 expressions in lung tissues of mice ($n = 8$).

	Group	Day 7	Day 10	Day 14
HIF-1a	C group	168.28 ± 3.64	173.60 ± 3.39	190.06 ± 3.58
	T1 group	$146.08 \pm 1.77^*$	$139.13 \pm 3.36^*$	$145.74 \pm 4.91^*$
	T2 group	$142.03 \pm 3.56^{*\triangle}$	$136.76 \pm 1.48^{*\triangle}$	$135.14 \pm 3.34^{*\triangle}$
VEGF	C group	142.49 ± 3.88	156.32 ± 2.35	165.21 ± 3.56
	T1 group	$125.53 \pm 5.19^*$	$113.97 \pm 4.00^*$	$105.85 \pm 1.65^*$
	T2 group	$94.53 \pm 2.84^{*\triangle}$	$86.95 \pm 3.02^{*\triangle}$	$63.59 \pm 2.39^{*\triangle}$
ET-1	C group	295.58 ± 4.83	299.95 ± 7.17	313.79 ± 6.79
	T1 group	$272.07 \pm 3.65^*$	$246.58 \pm 3.18^*$	$195.81 \pm 2.59^*$
	T2 group	$243.67 \pm 3.73^{*\triangle}$	$211.63 \pm 4.77^{*\triangle}$	$165.17 \pm 2.93^{*\triangle}$

Compared with the C group, $^*P < 0.001$; compared with the T1 group, $^\triangle P < 0.001$.

Table 5. Correlation of HIF-1a, VEGF, and ET-1 expression in the treatment group.

Indicators	Day 7		Day 10		Day 14	
	r	P	r	P	r	P
HIF-1a and VEGF	0.818*	< 0.001	0.924*	< 0.001	0.961*	< 0.001
HIF-1a and ET-1	0.927*	< 0.001	0.925*	< 0.001	0.983*	< 0.001
VEGF and ET-1	0.941*	< 0.001	0.988*	< 0.001	0. 976*	< 0.001

*Correlation coefficient, $P < 0.001$.

Table 6. Mean absorbance ratio of the mRNA of HIF-1a, VEGF, and ET-1 in the lung tissue ($n = 8$).

	Group	Day 7	Day 10	Day 14
HIF-1a	C group	3.89 ± 0.54	5.62 ± 0.61	8.13 ± 0.74
	T1 group	$5.93 \pm 0.37^*$	$3.66 \pm 1.04^*$	$3.68 \pm 0.64^*$
	T2 group	$4.47 \pm 0.70^{*\triangle}$	$3.39 \pm 0.99^{*\triangle}$	$3.43 \pm 0.61^{*\triangle}$
VEGF	C group	1.42 ± 0.16	1.75 ± 0.24	2.29 ± 0.04
	T1 group	$2.24 \pm 0.21^*$	$1.52 \pm 0.06^*$	$1.49 \pm 0.14^*$
	T2 group	$1.68 \pm 0.23^{*\triangle}$	$1.47 \pm 0.07^{*\triangle}$	$1.14 \pm 0.06^{*\triangle}$
ET-1	C group	3.11 ± 0.76	2.90 ± 0.99	5.38 ± 0.93
	T1 group	$3.54 \pm 0.43^*$	$2.61 \pm 0.62^*$	$2.87 \pm 0.56^*$
	T2 group	$2.35 \pm 0.33^{*\triangle}$	$2.06 \pm 0.46^{*\triangle}$	$2.07 \pm 0.47^{*\triangle}$

Compared with the C group, $^*P < 0.001$; compared with the T1 group, $^\triangle P < 0.001$.

3.6 Correlation of the mRNA level of HIF-1a, VEGF, and ET-1 in lung tissues of the treated group

HIF-1a mRNA level was positively correlated with VEGF mRNA or ET-1 mRNA, and VEGF mRNA was positively correlated with ET-1 mRNA (Table 7).

4 DISCUSSION

In our study, CIH mice were treated with different doses of ginsenoside Rg1 and the results showed that the expression of HIF-1a, VEGF, and ET-1 was significantly reduced with the higher dose being more effective than the low dose, indicating that ginsenoside Rg1 might be used for the treatment of CIH-induced lung injury.

The possible mechanisms of ginsenoside Rg1's effect might be the following. (1) Possibly through regulation of the pulmonary artery smooth muscle cells, calcium pool modulates calcium influx. Intracellular calcium exerts an effect on dilating blood vessels in order to improve the local tissue hypoxia. Intracellular reactive oxygen species (ROS) is the initiating factor for the upregulated levels of transcription factors in vascular endothelial cells and can cause further activation of proline hydroxylase (prolylhydroxylase, PHD), which enables the rapid degradation of HIF-1a *in vivo*, leading to reduced expression of the downstream target genes VEGF and ET-1 (Truty et al., 2021; Yang et al., 2022). (2) K^+ channels play a role in maintaining the stable potential of vascular smooth muscle cells and regulating the balance of free calcium ion concentration (Maniscalco et al., 2016; Tyrrell et al., 2016). There are four K^+ channels on pulmonary vascular smooth muscle cells: ATP-sensitive potassium (mitoKATP), Ca^{2+}-activated potassium (K_{Ca}), voltage-gated potassium (K_v), and internal rectifier potassium (K_{ir}). Ginsenoside Rg1 may inhibit mitochondrial mitoKATP that controls mitochondrial membrane potential, downregulate H_2O_2 production by mitochondria, and further inhibit the expression of HIF-1a. (3) Release of NO and prostacyclin can inhibit the expression of endothelin convertase (Domann et al., 2000; Duan et al., 2011; Duong et al., 2016; Eisenhauer et al., 2009). Ginsenoside Rg1 can also upregulate NOS mRNA expression and promote NO production (Grimm et al., 2020; Tang & Zhang, 2020). NO is generated by the amino acid L-arginine and its activation in vascular smooth muscle cells causes a massive increase in guanosine phosphate in inner cells (Ding et al., 2011). NO can also inhibit ET-1 and phospholipase C and A2 and protein kinase C, including c-fos, c-jun, and c-myc. Promotion of the NO synthesis inhibits ET-1 synthesis and release and pulmonary vasoconstriction as well as vascular remodeling due to active factors .

Table 7. Correlation analysis of HIF-1a mRNA, VEGF mRNA, and ET-1 mRNA expression in the lung tissues of the treated group.

Indicators	Day 7		Day 10		Day 14	
	r	P	r	P	r	P
HIF-1a and VEGF	0.640*	0.001	0.513*	0.010	0.781*	< 0.001
HIF-1a and ET-1	0.356	0.087	0.329	0.117	0.779*	< 0.001
VEGF and ET-1	0.514*	0.010	-0.138	0.521	0.649*	0.001

*Correlation coefficient, $P < 0.05$ or $P < 0.001$.

In conclusion, ginsenoside Rg1 can inhibit the expression of HIF-1a, VEGF, and ET-1 and therefore might improve the damage of pulmonary arterioles induced by CIH, indicating that it might be used as a novel treatment approach for treating lung injury induced by CIH.

REFERENCES

Ajoolabady, A., Kaplowitz, N., Lebeaupin, C., Kroemer, G., Kaufman, R. J., Malhi, H., & Ren, J. (2023). Endoplasmic reticulum stress in liver diseases. *Hepatology, 77*(2), 619-639. https://doi.org/10.1002/hep.32562

Akatsuka, Y. (2020). TCR-Like CAR-T Cells Targeting MHC-Bound Minor Histocompatibility Antigens. *Frontiers in Immunology, 11*, 257. https://doi.org/10.3389/fimmu.2020.00257

Amsen, D., Blander, J. M., Lee, G. R., Tanigaki, K., Honjo, T., & Flavell, R. A. (2004). Instruction of distinct CD4 T helper cell fates by different notch ligands on antigen-presenting cells. *Cell, 117*(4), 515-526. https://doi.org/10.1016/s0092-8674(04)00451-9

An, L., Liu, C. T., Qin, X. B., Liu, Q. H., Liu, Y., & Yu, S. Y. (2011). Protective effects of hemin in an experimental model of ventilator-induced lung injury. *European Journal of Pharmacology, 661*(1-3), 102-108. https://doi.org/10.1016/j.ejphar.2011.04.032

Antonarakis, E. S., Lu, C., Wang, H., Luber, B., Nakazawa, M., Roeser, J. C., Chen, Y., Mohammad, T. A., Chen, Y., Fedor, H. L., Lotan, T. L., Zheng, Q., De Marzo, A. M., Isaacs, J. T., Isaacs, W. B., Nadal, R., Paller, C. J., … & Luo J. (2014). AR-V7 and resistance to enzalutamide and abiraterone in prostate cancer. *New England Journal of Medicine, 371*(11), 1028-1038. https://doi.org/10.1056/NEJMoa1315815

Askenase, P. W. (2021). Ancient Evolutionary Origin and Properties of Universally Produced Natural Exosomes Contribute to Their Therapeutic Superiority Compared to Artificial Nanoparticles. *International Journal of Mollecular Science, 22*(3), 1429. https://doi.org/10.3390/ijms22031429

Aversa, S., Marseglia, L., Manti, S., D'Angelo, G., Cuppari, C., David, A., Chirico, G., & Gitto, E. (2016). Ventilation strategies for preventing oxidative stress-induced injury in preterm infants with respiratory disease: an update. *Paediatric Respiratory Reviews, 17*, 71-79. https://doi.org/10.1016/j.prrv.2015.08.015

Baimas-George, M., Watson, M., Murphy, K. J., Sarantou, J., Vrochides, D., Martinie, J. B., Baker, E. H., Mckillop, I. H., & Iannitti, D. A. (2021). Treatment of spontaneously ruptured hepatocellular carcinoma: use of laparoscopic microwave ablation and washout. *HPB, 23*(3), 444-450. https://doi.org/10.1016/j.hpb.2020.08.001

Ding, D. P., Chen, Z. L., Zhao, X. H., Wang, J. W., Sun, J., Wang, Z., Tan, F. W., Tan, X. G., Li, B. Z., Zhou, F., Shao, K., Li, N., Qiu, B., & He, J. (2011). miR-29c induces cell cycle arrest in esophageal squamous cell carcinoma by modulating cyclin E expression. *Carcinogenesis, 32*(7), 1025-1032. https://doi.org/10.1093/carcin/bgr078

Dłuski, D. F., Ruszała, M., Rudziński, G., Pożarowska, K., Brzuszkiewicz, K., & Leszczyńska-Gorzelak, B. (2022). Evolution of Gestational Diabetes Mellitus across Continents in 21st Century. *International Journal of Environmental Research and Public Health, 19*(23), 15804. https://doi.org/10.3390/ijerph192315804

Domann, F. E., Rice, J. C., Hendrix, M. J., & Futscher, B. W. (2000). Epigenetic silencing of maspin gene expression in human breast cancers. *International Journal of Cancer, 85*(6), 805-810. https://doi.org/10.1002/(sici)1097-0215(20000315)85:6%3C805::aid-ijc12%3E3.0.co;2-5

Duan, Z., Choy, E., Harmon, D., Liu, X., Susa, M., Mankin, H., & Hornicek, F. (2011). MicroRNA-199a-3p is downregulated in human osteosarcoma and regulates cell proliferation and migration. *Mollecular Cancer Therapeutics*, *10*(8), 1337-1345. https://doi.org/10.1158/1535-7163.mct-11-0096

Duong, V., Mey, C., Eloit, M., Zhu, H., Danet, L., Huang, Z., Zou, G., Tarantola, A., Cheval, J., Perot, P., Laurent, D., Richner, B., Ky, S., Heng, S., Touch, S., Sovann, L., van Doorn, R., … & Buchy, P. (2016). Molecular epidemiology of human enterovirus 71 at the origin of an epidemic of fatal hand, foot and mouth disease cases in Cambodia. *Emerging Microbes & Infectious*, *5*(9), e104. https://doi.org/10.1038/emi.2016.101

Eisenhauer, E. A., Therasse, P., Bogaerts, J., Schwartz, L. H., Sargent, D., Ford, R., Dancey, J., Arbuck, S., Gwyther, S., Mooney, M., Rubinstein, L., Shankar, L., Dodd, L., Kaplan, R., Lacombe, D., Verweij, J. (2009). New response evaluation criteria in solid tumours: revised RECIST guideline (version 1.1). *European Journal of Cancer*, *45*(2), 228-247. https://doi.org/10.1016/j.ejca.2008.10.026

Galluzzi, L., Humeau, J., Buqué, A., Zitvogel, L., & Kroemer, G. (2020). Immunostimulation with chemotherapy in the era of immune checkpoint inhibitors. *Nature Reviews Clinical Oncology*, *17*(12), 725-741. https://doi.org/10.1038/s41571-020-0413-z

Grimm, D., Bauer, J., Wise, P., Krüger, M., Simonsen, U., Wehland, M., Infanger, M., & Corydon, T. J. (2020). The role of SOX family members in solid tumours and metastasis. *Seminars in Cancer Biology*, *67*(Pt 1), 122-153. https://doi.org/10.1016/j.semcancer.2019.03.004

Huang, H., Qiu, Y., Huang, G., Zhou, X., Zhou, X., & Luo, W. (2019). Value of Ferritin Heavy Chain (FTH1) Expression in Diagnosis and Prognosis of Renal Cell Carcinoma. *Medical Science Monitor*, *25*, e914162. https://doi.org/10.12659/msm.914162

Huang, J., Hu, Y., Jiang, H., Xu, Y., Lu, S., Sun, F., Zhu, J., Wang, J., Sun, X., Liu, J., Zhen, Z., & Zhang, Y. (2020). CHIC Risk Stratification System for Predicting the Survival of Children With Hepatoblastoma: Data From Children With Hepatoblastoma in China. *Frontiers in Oncology*, *10*, 552079. https://doi.org/10.3389/fonc.2020.552079

Jeon, J. H., Im, S., Kim, H. S., Lee, D., Jeong, K., Ku, J. M., & Nam, T. G. (2022). Chemical Chaperones to Inhibit Endoplasmic Reticulum Stress: Implications in Diseases. *Drug Design, Development and Therapy*, *16*, 4385-4397. https://doi.org/10.2147/dddt.S393816

Maniscalco, M., Paris, D., Melck, D. J., D'Amato, M., Zedda, A., Sofia, M., Stellato, C., & Motta, A. (2016). Coexistence of obesity and asthma determines a distinct respiratory metabolic phenotype. *Journal of Allergy and Clinical Immunology*, *139*(5), 1536-1547. e5. https://doi.org/10.1016/j.jaci.2016.08.038

Perner, C., & Krüger, E. (2022). Endoplasmic Reticulum Stress and Its Role in Homeostasis and Immunity of Central and Peripheral Neurons. *Frontiers in Immunology*, *13*, 859703. https://doi.org/10.3389/fimmu.2022.859703

Poher, A. L., Tschöp, M. H., & Müller, T. D. (2018). Ghrelin regulation of glucose metabolism. *Peptides*, *100*, 236-242. https://doi.org/10.1016/j.peptides.2017.12.015

Tang, L., & Zhang, X. M. (2020). Serum TSGF and miR-214 levels in patients with hepatocellular carcinoma and their predictive value for the curative effect of transcatheter arterial chemoembolization. *Annals of Palliative Medicine*, *9*(4), 2111-2117. https://doi.org/10.21037/apm-20-1224

Truty, M. J., Kendrick, M. L., Nagorney, D. M., Smoot, R. L., Cleary, S. P., Graham, R. P., Goenka, A. H., Hallemeier, C. L., Haddock, M. G., Harmsen, W. S., Mahipal, A., McWilliams, R. R., Halfdanarson, T. R., & Grothey, A. F. (2021). Factors Predicting Response, Perioperative Outcomes, and Survival Following Total Neoadjuvant Therapy for Borderline/Locally Advanced Pancreatic Cancer. *Annals of Surgery*, *273*(2), 341-349. https://doi.org/10.1097/sla.0000000000003284

Tyrrell, J., Richmond, R. C., Palmer, T. M., Feenstra, B., Rangarajan, J., Metrustry, S., Cavadino, A., Paternoster, L., Armstrong, L. L., De Silva, N. M., Wood, A. R., Horikoshi, M., Geller, F., Myhre, R., Bradfield, J. P., Kreiner-Møller, E., Huikari, V., … & Early Growth Genetics (EGG) Consortium (2016). Genetic Evidence for Causal Relationships Between Maternal Obesity-Related Traits and Birth Weight. *Jama*, *315*(11), 1129-1140. https://doi.org/10.1001/jama.2016.1975

Versteijne, E., Suker, M., Groothuis, K., Akkermans-Vogelaar, J. M., Besselink, M. G., Bonsing, B. A., Buijsen, J., Busch, O. R., Creemers, G. M., van Dam, R. M., Eskens, F. A. L. M., Festen, S., de Groot, J. W. B., Groot Koerkamp, B., de Hingh, I. H., Homs, M. Y. V., van Hooft, J. E., … & Dutch Pancreatic Cancer Group. (2020). Preoperative Chemoradiotherapy Versus Immediate Surgery for Resectable and Borderline Resectable Pancreatic Cancer: Results of the Dutch Randomized Phase III PREOPANC Trial. *Journal of Clinical Oncology*, *38*(16), 1763-1773. https://doi.org/10.1200/jco.19.02274

Yang, C. Y., Lin, R. T., Chen, C. Y., Yeh, C. C., Tseng, C. M., Huang, W. H., Lee, T.-Y., Chu, C.-S., & Lin, J. T. (2022). Accuracy of simultaneous measurement of serum biomarkers: Carbohydrate antigen 19-9, pancreatic elastase-1, amylase, and lipase for diagnosing pancreatic ductal adenocarcinoma. *Journal of the Formosan Medical Association*, *121*(12), 2601-2607. https://doi.org/10.1016/j.jfma.2022.07.003

Zaibi, N., Li, P., & Xu, S. Z. (2021). Protective effects of dapagliflozin against oxidative stress-induced cell injury in human proximal tubular cells. *PLoS One*, *16*(2), e0247234. https://doi.org/10.1371/journal.pone.0247234